

Supplementary methods

Optimizing topic model parameters

In order to create accurate episode and recall models, we used an optimization method that was driven by our ability to explain hand-annotated memory performance metrics collected by Chen et al. (2017). In an earlier variant of our study (Heusser and Manning, 2018), we used a grid search to compute the ω (episode sliding window duration, in scenes), ρ (recall sliding window duration, in sentences), and K (number of topics) that satisfied

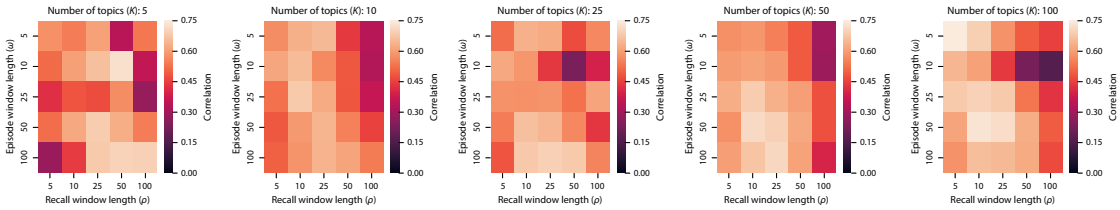
$$\operatorname{argmax}_{\omega, \rho, K} [\operatorname{corr}(\operatorname{corr}(\mu(\omega, \rho, K), v(\omega, \rho, K)), \theta)],$$

where $\operatorname{corr}(\mu, v)$ is the per-participant correlation between the episode (μ) and recall (v) topic proportions matrices, and θ is the per-participant hand-counted number of recalled scenes. We searched over a grid of pre-specified values for each of these parameters; the resulting correlations are displayed in Figure 1. The optimal parameters were $\omega = 50$, $\rho = 10$, and $K = 100$. In our current paper we made a number of improvements to how we preprocessed text and fit topic models (see *Methods*), but we carried the same optimal parameters forward from Heusser and Manning (2018) without performing any additional optimization.

The optimized model converged on 32 unique topics that were assigned non-zero weights. We provide a list of the top ten highest-weighted words from each topic in Figure 2.

Feature importance analyses

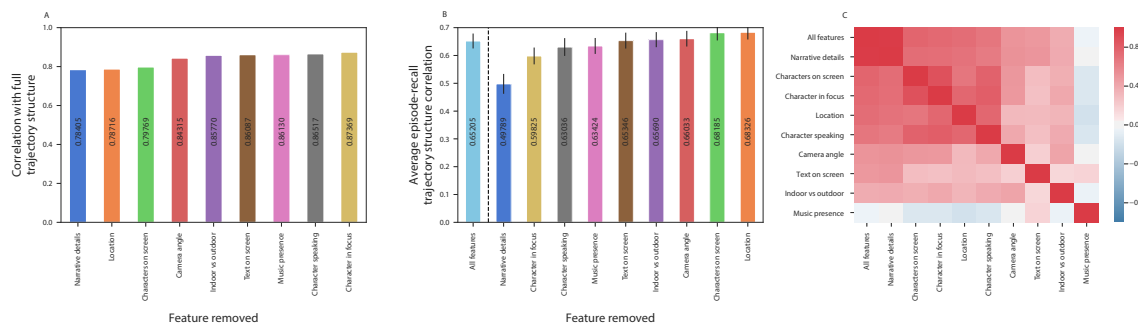
To determine the contribution of each feature to the temporal structure of the episode topic proportions matrix, we conducted a “leave one out” analysis. Specifically, we compared the original episode’s topic proportions matrix (created using all hand-annotated features from the 998 manually identified scenes spanning the *Sherlock* episode; see *Methods* for a full list of features) with topic proportions matrices created using all but one type of feature. For each impoverished topic proportions matrix, we computed the timepoint-by-timepoint correlation matrix, and correlated the proximal diagonals from the upper triangle with those from the temporal correlation matrix of the feature-complete matrix (for details on how we isolated proximal temporal correlations, see *Methods*). Observing a lower correlation between an impoverished matrix (with a particular



Supplementary Figure 1: Optimizing topic model parameters. We performed a grid search over episode sliding window length ($\omega \in \{5, 10, 25, 50, 100\}$), recall sliding window length ($\rho \in \{5, 10, 25, 50, 100\}$), and number of topics ($K \in \{5, 10, 25, 50, 100\}$). The reported correlations are between per-participant episode-recall correlations and per-participant hand-counted numbers of recalled scenes.

Topic ID	Top 10 words	Topic description
1	john, outdoor, yes, phone, road, brixton, box, medium, donovan, street	John being watched
2	sherlock, john, indoor, laboratory, hospital, st, bartholomew, medium, yes, mike	Sherlock and John meet
4	man, john, warehouse, indoor, yes, medium, shoulder, says, hand, asks	Meeting with Mycroft
5	john, mike, sherlock, medium, molly, park, russell, square, outdoor, bench	Running into an old friend
7	yes, jeffrey, sir, jimmy, indoor, aide, medium, helen, woman, gary	First and second murder
9	sherlock, floor, room, crime, scene, lauriston, indoor, gardens, john, yes	Examining the body (a)
17	sherlock, lestrade, john, indoor, gardens, lauriston, room, medium, floor, scene	Lestrade calls in Sherlock (a)
20	soldiers, singers, cartoon, background, medium, indoor, world, yes, afghanistan, lobby	Intro cartoon/War flashback
22	sherlock, john, street, baker, 221b, indoor, mrs, hudson, suite, yes	221B Baker St. (a)
27	sherlock, john, outdoor, medium, taxi, road, yes, says, phone, lauriston	Sherlock analyzes John (a)
28	sherlock, john, lestrade, lauriston, gardens, medium, anderson, donovan, indoor, yes	Who was Rachel?
30	sherlock, john, indoor, mediu, baker, street, 221b, suite, yes, phone	John texts the killer
32	donovan, lestrade, indoor, medium, aide, jimmy, press, room, conference, yes	Press conference (a)
35	john, sherlock, street, baker, medium, says, indoor, mrs, hudson, sequence	John leaves the flat
37	sherlock, john, street, suite, 221b, baker, indoor, medium, says, asks	221B Baker St. (b)
40	sherlock, lestrade, yes, room, gardens, indoor, lauriston, floor, john, scene	Examining the body (b)
42	sherlock, molly, john, bartholomew, st, hospital, medium, indoor, mike, room	John meets Sherlock Holmes
46	singers, cartoon, background, indoor, world, lobby, popcorn, yes, people, medium	Intro cartoon
48	john, donovan, gardens, lauriston, yes, street, outdoor, medium, shoulder, policeman	Unpopular with the police (a)
65	lestrade, donovan, indoor, room, press, conference, police, reporter, medium, reporters	Press conference (b)
68	john, medium, anthea, yes, indoor, street, baker, sherlock, outdoor, man	Kidnapping John
70	john, man, yes, warehouse, indoor, medium, shoulder, says, anthea, continues	Anthea brings John to Mycroft
72	sherlock, john, lestrade, lauriston, gardens, medium, indoor, yes, stairway, stairs	Lestrade calls in Sherlock (b)
73	jimmy, yes, sir, jeffrey, indoor, medium, gary, psychotherapist, helen, john	John's psychotherapist (a)
75	sherlock, john, donovan, outdoor, medium, gardens, lauriston, street, anderson, says	Unpopular with the police (b)
78	john, lestrade, mike, medium, donovan, indoor, park, room, conference, press	John takes a walk
80	john, sherlock, yes, indoor, laboratory, bartholomew, st, hospital, medium, mike	Sherlock analyzes John (b)
84	john, anthea, yes, road, man, outdoor, phone, medium, brixton, car	Anthea drives John home
85	sherlock, john, yes, taxi, outdoor, road, medium, says, phone, continues	Chasing the killer
87	john, indoor, jeffrey, sir, psychotherapist, medium, yes, room, london, helen	John's psychotherapist (b)
91	sherlock, john, lestrade, room, floor, crime, scene, gardens, lauriston, indoor	Examining the body (c)
93	john, room, indoor, medium, soldiers, psychotherapist, yes, outdoor, close, soldier	War flashback

Supplementary Figure 2: Topics discovered in *Sherlock*. We applied a topic model to hand-annotated information about 1000 scenes spanning the 48-minute episode. We identified 32 unique topics with non-zero weights (we used $K = 100$ topics to fit the model). Each topic comprises a distribution of weights over all words in the vocabulary. For each topic, we show the words with the 10 largest weights, along with a suggested description of the topic.



Supplementary Figure 3: Feature importance analysis. **A.** Contributions of each feature type to the structure of the episode topic proportions matrix. The bar heights reflect the correlation between the proximal temporal structure (see *Methods*) of the episode topic proportions matrix computed using all features, and that of an episode topic proportions matrix computed using all features except the indicated feature. Lower bars reflect features that contribute more substantially to the episode’s temporal structure. **B.** Which features are preserved during recall? The bar heights reflect the (average) across-participant correlations between the proximal temporal structure of episode and recall topic proportions matrices constructed in the absence of the given feature. Error bars denote standard error of the mean. **C.** Feature correlation matrix. Each entry displays the correlation between episode topic portions matrices created using only the indicated (row/column) features.

feature removed) and the feature-complete matrix would suggest that the held-out feature contributed more prominently to the full episode topic proportion matrix’s temporal structure. We found that hand-annotated narrative details played the greatest roll in determining the temporal structure of the episode, whereas the name of the character(s) in focus for each shot contributed least (Fig. 3A).

Next, we sought to determine which annotated features contributed aspects of the episode’s temporal structure that were preserved in participants’ later recalls. Specifically, we computed the timepoint-by-timepoint correlation matrix of the episode’s topic proportions matrix, and correlated the proximal diagonals from its upper triangle with those from the timepoint-by-timepoint correlation matrices for each participant’s recall topic proportions matrices (stretched via linear interpolation to have the same number of timepoints as the episode topic proportions matrix). This yielded a single correlation coefficient for each participant. We then repeated this analysis with each annotated feature held out in turn. Observing a lower correlation between the episode and recall topic proportions matrices (constructed in the absence of a given feature) would indicate that participants utilize changes in that feature’s content to discriminate between sections of the episode when organizing their recalls. We found that hand-annotated narrative details were the most heavily utilized feature, whereas changes in the text present on-screen, the indoor/outdoor distinction between shots, the camera angle, the names of the various characters on screen, and the shot’s location tended not to impact participants’ recall structures (i.e., removing those features resulted in a *greater* episode-recall correlation than including them; Fig. 3B).

We also wondered how the different types of features might relate. For example, knowing which character is in focus during a given scene may also provide information about which character is speaking. We computed topic proportions matrices from the annotations for each individual feature, in turn, and (using the same technique as in the above analyses) compared

the proximal temporal correlation structure of each single-feature topic proportions matrix to each other, as well as to that of the full episode. This provided additional confirmation that the full episode’s temporal structure was largely driven by narrative details. We also found that character-driven features (characters on screen, characters speaking, and characters in focus) were strongly correlated. Other details, such as the presence or absence of music, led to very different topic proportions matrices (Fig. 3C).

Creating a low-dimensional embedding space

Figures 6 and 7C in the main text display two-dimensional projections of the 100-dimensional topic trajectories for the episode (Figs. 6A, 7C), average recall (Fig. 6B), and each individual’s recall (Figs. 6C, 7C). We created these embeddings using the Uniform Manifold Approximation and Projection algorithm (UMAP; McInnes et al., 2018) called from our high-dimensional visualization and text analysis software, *HyperTools* (Heusser et al., 2018). An advantage of the UMAP algorithm over comparable manifold learning techniques (e.g., *t*-SNE) is that UMAP explicitly attempts to preserve the global structure of the data (McInnes et al., 2018; Becht et al., 2019) by constructing a space where distance on the manifold is standard Euclidean distance, with respect to the global coordinate system. This was important in our use case, as we wanted to visualize both the evolving structure of the episode and the spatial relationships between presented and recalled content.

UMAP achieves a balance between representing local and global structure via a subset of its hyperparameters: `n_neighbors`, `spread`, and `min_dist`. The `n_neighbors` hyperparameter (K) denotes the number of nearest neighbors to consider in constructing the high-dimensional fuzzy simplicial set for each datapoint. The `spread` (γ) and `min_dist` (δ) hyperparameters function together to create the differentiable decay curve used to approximate the injective function for mapping between high- and low-dimensional fuzzy simplicial sets. In brief, `min_dist` determines the degree to which nearby points are clustered or expanded, relative to the overall `spread`.

Two other parameters ultimately affect this balance between preserving local versus global structure: the seed (τ) for the (pseudo-)random number generator (RNG), and the order of the observations (i.e., trajectories) to be embedded (φ). As described in *Methods*, we ensured the episode and recall events were projected onto the *same* low-dimensional manifold by fitting the embedding model to a stacked matrix of all episode, average recall, and individuals’ recall events. After initializing the low-dimensional simplicial set (by default, using a spectral embedding of the high-dimensional simplicial set’s fuzzy 1-skeleton), UMAP optimizes the embedding using stochastic gradient descent with cross-entropy as a cost function. During optimization, indices of the data are sampled at random, and thus the local minimum achieved by the optimization is dependent on both the state of the RNG and the sequence in which observations are concatenated.

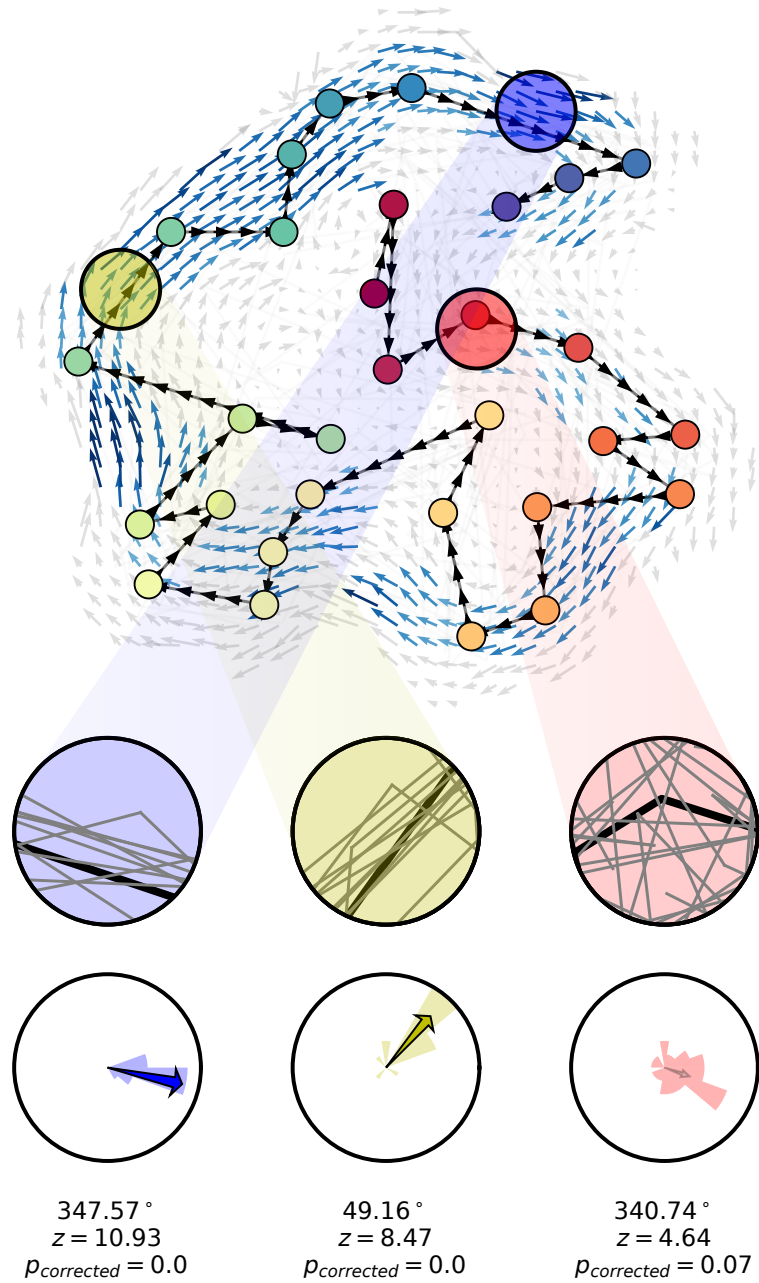
We performed a grid search over pre-specified values of these hyperparameters, and optimized the manifold space for visualization based on two criteria. First, the 2D embedding of the episode trajectory should reflect its original 100-dimensional structure as faithfully as possible. Second, the path traversed by the embedded episode trajectory should intersect itself a minimal number of times. The first criteria helps bolster the validity of visual intuitions about relationships between sections of episode content, based on their locations in the embedding space. The second criteria was motivated by the observed low off-diagonal values in the episode topic proportions matrix’s temporal correlation matrix (suggesting that the same topic-space coordinates should not be re-visited; see Figure 2A in the main text). Further, we found through simulation that our statistical procedure for testing the consistency of trajectory directions across participants (Fig. 6B, also see

Methods) can be confounded when and where the topic trajectory intersects itself. We formalized this optimization as the combination of hyperparameter values that satisfied

$$\begin{aligned} & \operatorname{argmax}_{\{K, \gamma, \delta, \tau, \varphi \in E \mid \Phi(K, \gamma, \delta, \tau, \varphi)\}} \left[\operatorname{corr}(\Upsilon(\xi_{K, \gamma, \delta, \tau, \varphi}), \Upsilon(\chi)) \right], \text{ where} \\ & \Phi(K, \gamma, \delta, \tau, \varphi) = \operatorname{argmin}_{K, \gamma, \delta, \tau, \varphi} \left[\Gamma(\xi_{K, \gamma, \delta, \tau, \varphi}) \right], \end{aligned}$$

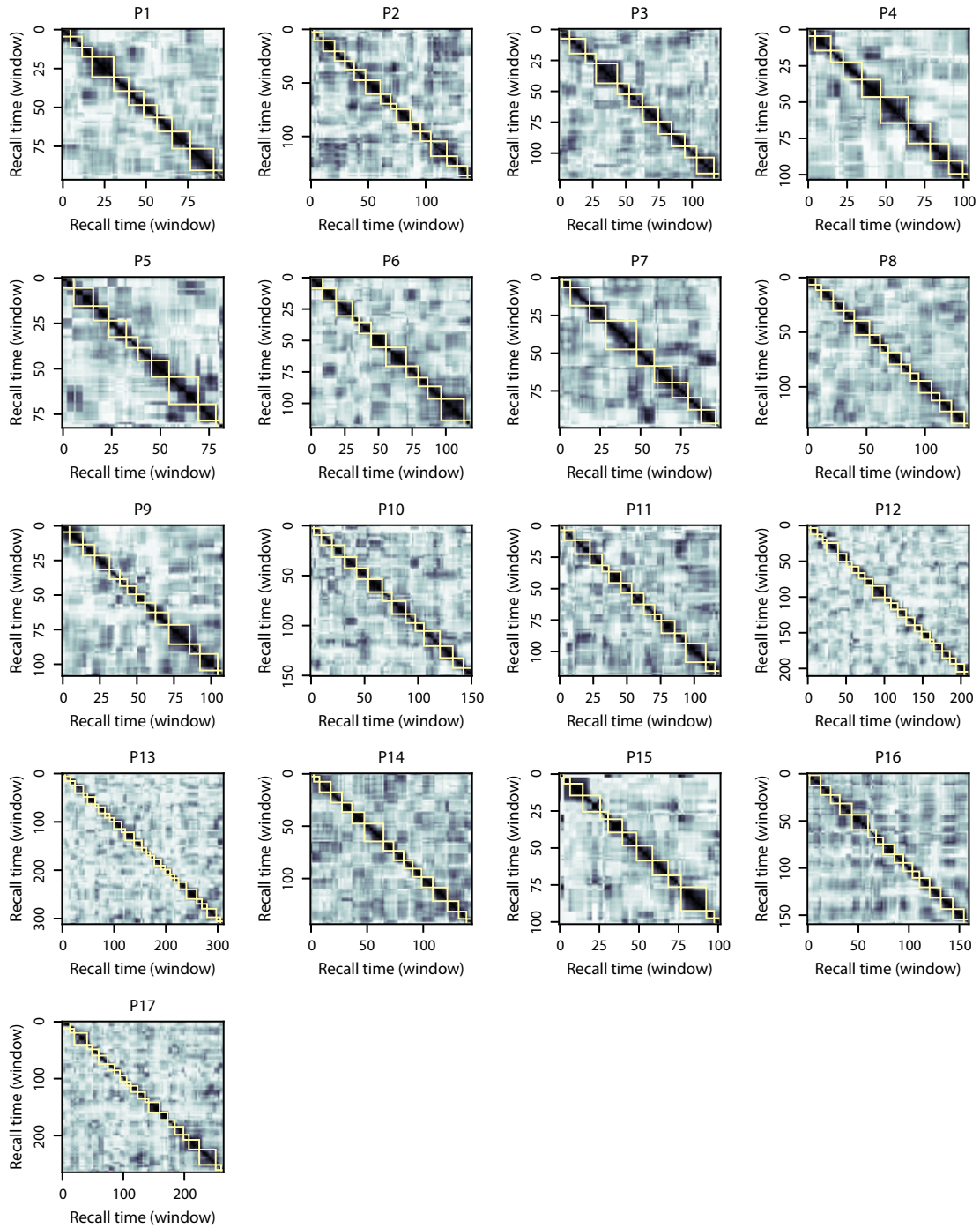
ξ is the episode’s trajectory through the manifold space; χ is the original, 100-dimensional episode trajectory; Υ is a function that computes a condensed matrix of pairwise distances between event vectors (computed using correlation distance in the original topic space and Euclidean distance in the manifold space); $\operatorname{corr}(\Upsilon(\xi), \Upsilon(\chi))$ is the correlation between the sets of pairwise distances, and Γ is the number of instances in which lines drawn between consecutive episode event embeddings intersected each other. The sets of hyperparameter values we searched over comprised: $K \in \{10x \in \mathbb{Z} \mid 10 < x < 22\} \cup \{161\}$ (a range roughly centered on half the total number of events, 161, in order to balance representations of local and global structure); $\gamma \in \{1, 3, 5, 7, 9\}$; $\delta \in \{0.1, 0.3, 0.5, 0.7, 0.9\}$; $\tau \in \{x \in \mathbb{Z} \mid 0 < x < 101\}$; and $\varphi \in \binom{S}{3}$, where $S = \{\text{episode events, average recall events, individual recall events}\}$. The optimal parameters (that yielded $\Phi = 0$) were $K = 170$, $\gamma = 7$, $\delta = 0.7$, $\tau = 41$, with the order of sequence φ as the average recall events, episode events, and individuals’ recall events, vertically concatenated, in order.

Supplementary figures

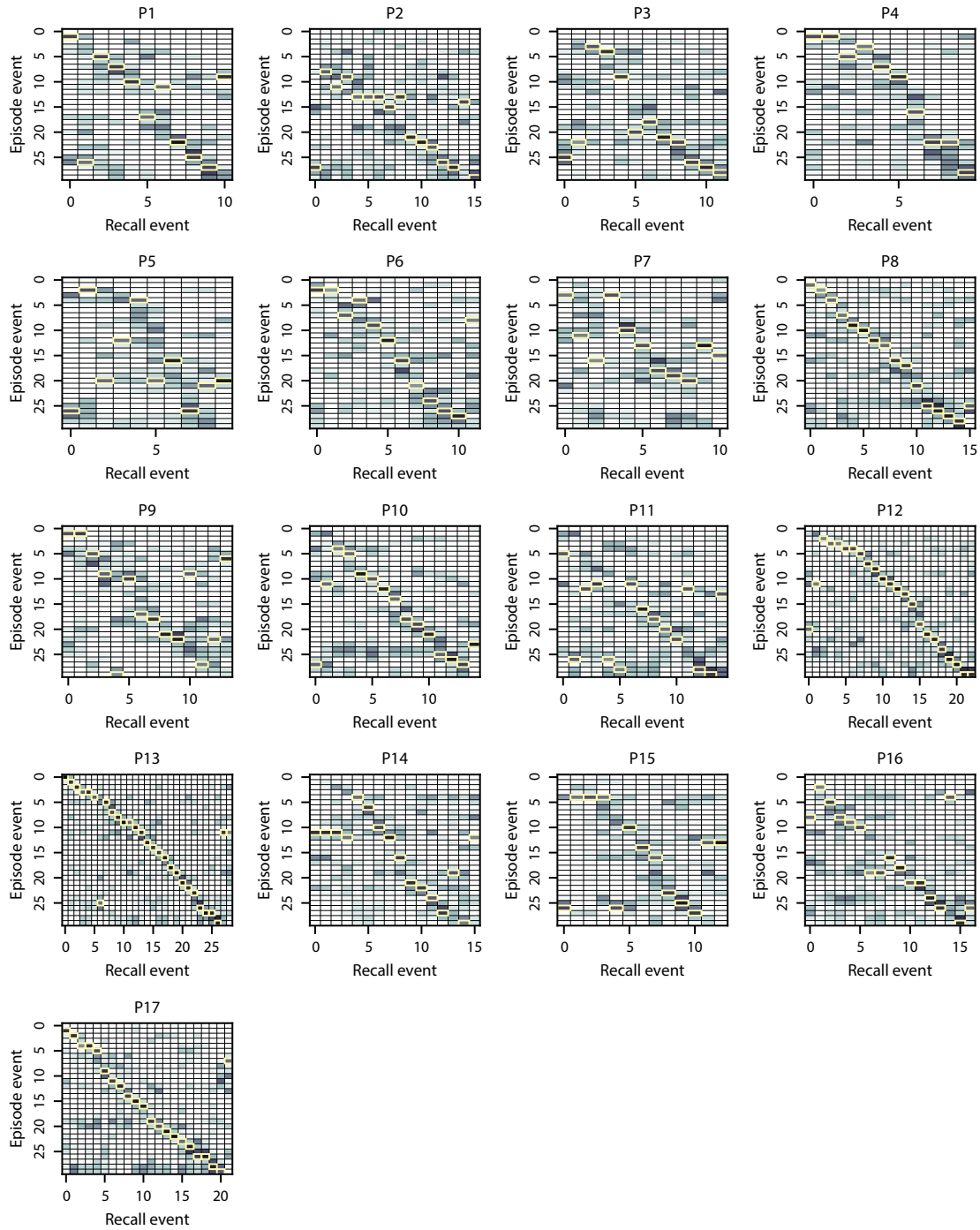


Supplementary Figure 4: Methods detail for recall trajectory analysis displayed in Figure 6B A. This panel replicates Figure 6B in the *Main text*, but with two additions. First, individual participants' recall trajectories are displayed (faintly) as light gray lines. Second, three locations on the trajectory have been highlighted (blue, yellow, and red circles). **B.** These zoomed-in views of the locations highlighted in Panel A show the average trajectory (black) and individual participants' trajectories (gray lines) that intersect the given region of topic space. **C.** For each circular region of topic space tiling the 2D embedding plane displayed in Panel A, we compute the distribution of angles formed between each participant's trajectory segment (i.e., the point at which the trajectory enters and exists the region of topic space) and the x -axis. The distributions of angles for these three example regions are displayed in the colored rose plots. We use Rayleigh tests to assign an arrow direction, length, and color for that region of topic space. Arrows displayed in blue are significant at the $p < 0.05$ level (corrected). The arrow directions are oriented according to the circular means of each distribution, and the arrow lengths are proportional to the lengths of those mean vectors. The example regions have been oriented from left to right in decreasing order of consistency across participants.

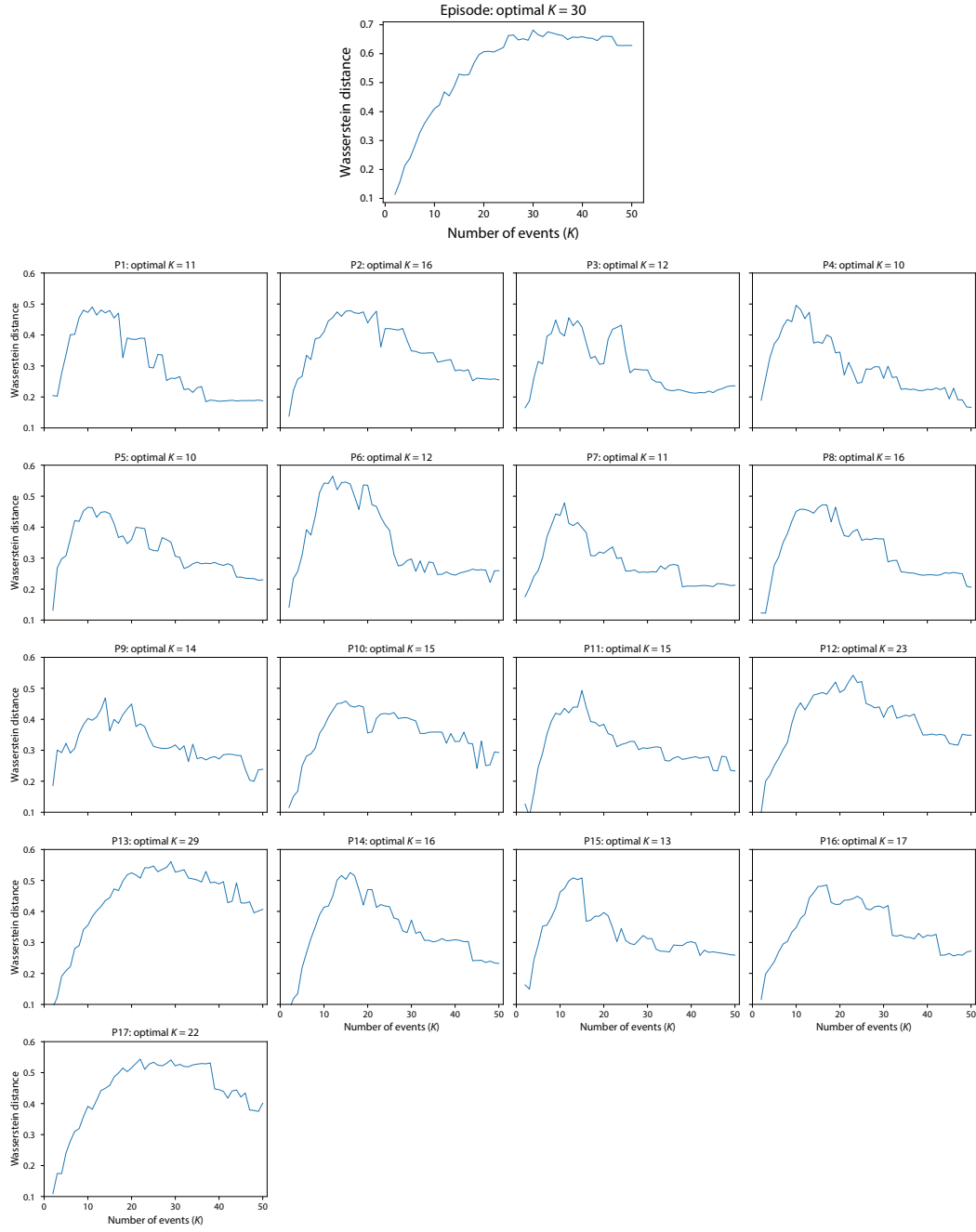
Participant-level figures referenced in the main text



Supplementary Figure 5: Recall temporal correlation matrices and event segmentation fits. Each panel is in the same format as Figure 2E in the main text. The yellow boxes indicate HMM-identified event boundaries.



Supplementary Figure 6: Episode-recall event correlation matrices. Each panel is in the same format as Figure 2G in the main text. The yellow boxes mark the matched episode event for each recall event (i.e., the maximum correlation in each column).



Supplementary Figure 7: Episode and recall topic proportions matrix K -optimization functions. We selected the optimal K -value for the episode and each recall topic proportions matrix using the formula described in *Methods*. This computation resulted in a curve for each matrix, describing the Wasserstein distance between the distributions of within-event and across-event topic vector correlations, as a function of K .

Supplementary references

- Becht, E., McInnes, L., Healy, J., Dutertre, C., Kwok, I. W. H., Ng, L. G., Ginhoux, F., and Newell, E. W. (2019). Dimensionality reduction for visualizing single-cell data using umap. *Nature biotechnology*, 37(1):38.
- Chen, J., Leong, Y. C., Honey, C. J., Yong, C. H., Norman, K. A., and Hasson, U. (2017). Shared memories reveal shared structure in neural activity across individuals. *Nature Neuroscience*, 20(1):115.
- Heusser, A. C. and Manning, J. R. (2018). Capturing the geometric structure of episodic memories for naturalistic experiences. In *Proceedings of the Conference on Cognitive Computational Neuroscience*, pages PS–2B.16.
- Heusser, A. C., Ziman, K., Owen, L. L. W., and Manning, J. R. (2018). HyperTools: a Python toolbox for gaining geometric insights into high-dimensional data. *Journal of Machine Learning Research*, 18(152):1–6.
- McInnes, L., Healy, J., and Melville, J. (2018). UMAP: Uniform manifold approximation and projection for dimension reduction. *arXiv*, 1802(03426).